*Original scientific paper*

# A comparison of pitting susceptibility of Q235 and HRB335 carbon steels used for reinforced concrete

GUOLIANG ZHAN, JIANCHENG LUO*, SHAOFEI ZHAO*, WEISHAN LI*✉

*New Century Concrete of Guangdong Foundation Co., Ltd, Guangzhou 510660, China*

**School of Chemistry and Environment, South China Normal University, Guangzhou 510006, China*

✉Corresponding Author: E-mail: liwsh@scnu.edu.cn; Tel.: +86-020-39310256; Fax: +86-020-39310256

### Abstract

*The phase structure and the pitting susceptibility of two carbon steels, Q235 and HRB335, used for reinforced concrete, are investigated by phase observation, polarization curve measure-ments, electrochemical impedance spectroscopy, and Mott-Schottky analysis. It is found that Q235 is ferrite and HRB335 is pearlite. Q235 is more susceptible to chloride ions leading to pit-ting than HRB335. The polarization curves show that the breakdown potential of the passive film in saturated Ca(OH)$_2$ solution containing 0.4 M NaCl is 0 V for Q235 and 0.34 V for HRB335. The Mott-Schottky analyses show that passive films formed on Q235 and HRB335 in saturated Ca(OH)$_2$ solution containing chloride ions behave like an n-type semiconductor. The passive film formed on Q235 has a higher donor density, which explains why Q235 is more susceptible to pitting than HRB335.*

### Keywords

Pitting susceptibility; Carbon steel; Phase structure; Polarization curve; Electrochemical impedance spectroscopy; Mott-Schottky.

## Introduction

Reinforced concrete is widely used as building material because the corrosion resistance of the embedded carbon steel for the reinforcement plays a significant role in the life of reinforced concrete. In a high quality concrete, the embedded carbon steel prevents corrosion by forming a passive film on a steel surface, which slows down the access of oxygen, moisture, and various aggressive species to the interface between steel and concrete [1]. Among all the aggressive species, chloride ions exhibit the strongest attack on passive film. Chloride ions may be introduced to the concrete from raw material, such as water and sand, or they can penetrate from the outside in highway viaducts where de-icing salts are used as well as in marine structures [2]. In practice,

the corrosive attack due to chloride penetration usually leads to pitting corrosion, which causes catastrophe because its initiation and propagation is difficult to predict.

The pitting susceptibility of carbon steel is related to the microstructure and composition of the steel and inhibitors used for the formation of passive films [3-12]. Various carbon steels usually are combined for use because of the need for strength and tenacity. For example, two kinds of carbon steels, Q235 and HRB335, are usually used together in reinforced concrete structures to improve the strength of concrete. It is necessary to understand the pitting susceptibility of various kinds of carbon steel for their successful application in reinforced concrete. The aim of this work is to understand the difference in pitting susceptibility between Q235 and HRB335.

**Experimental**

*Electrodes and solutions*

The composition of Q235 and HRB335 is given in Table 1. The steel specimens ($\phi$ 0.8 cm × 0.5 cm) were embedded in epoxy resin, with a test area of 0.5 cm$^2$. Prior to each measurement, the working surface of specimens was polished with different $SiC_2$ abrasive papers and $Al_2O_3$ powder of 0.05 μm, then degreased with ethanol and rinsed with de-ionized water successively.

The saturated $Ca(OH)_2$ solution was prepared as simulated concrete pore solution (SPS) with de-ionized water. NaCl was added to form the solution containing chloride ions. All the chemicals used were of analytical grade.

*Table 1. Composition of Q235 and HRB335, wt. %*

| Samples | C | Mn | P | S | Si | Cr | Ni | Al | As |
|---------|------|-------|-------|------|-------|-------|-------|-------|-------|
| Q235 | 0.15 | 0.326 | 0.039 | 0.03 | 0.115 | 0.024 | 0.032 | 0.127 | 0.028 |
| HRB335 | 0.26 | 0.698 | 0.046 | 0.05 | 0.324 | 0.033 | 0.039 | 0.016 | 0.026 |

*Phase-structure observation*

Optical microscope (ECLIPSE 50iPOL, Nikon Corporation) was used to observe the microstructure of Q235 and HRB335. Before the observation, the specimens were etched with 0.2 % Nital for 10s, degreased with ethanol and rinsed with de-ionized water.

*Electrochemical measurement*

The electrochemical measurements were carried out with PGSTAT-30 (Autolab, Eco Chemise B. V. Company). A classical three electrodes electrochemical cell was used. A platinum sheet with a geometric area of 1 cm$^2$ was used as the counter electrode and a saturated calomel electrode (SCE) was used as the reference electrode. All the potentials in this paper are versus the SCE.

The electrolyte was deareated with nitrogen for 30 min before each measurement, and all the electrochemical measurements were carried out at ambient temperature without stirring. The potential scanning rate used in the polarization curve measurements was 0.5 mV s$^{-1}$. The impedance measurements were carried out in frequency range from 100 kHz to 0.01 Hz. In the Mott-Schottky measurement, the frequency used was 1 kHz and the potential step was 5 mV. Prior to each measurement, the working electrode was firstly kept at -1.15 V for 30 min, then at 0 V for 60 min to form a passive film, and finally it was stabilized at open circuit potential (OCP) for 30 min.

## Results and Discussion

### Phase structure

Fig. 1 presents the phase structure of Q235 (A) and HRB335 (B). Both, Q235 and HRB335 have two phases, pearlite and ferrite [11,13]. However, the proportion of ferrite and pearlite is different in HRB335 and Q235. Ferrite phase prevails in Q235 while in HRB335 prevails mainly pearlite. The composition of two carbon steel is similar except for the contents of Mn and Si (Table 1), which might account for the difference in microstructure between two carbon steels. From the different microstructure of the two carbon steels, it can be expected that they exhibit different pitting susceptibility [3,9].
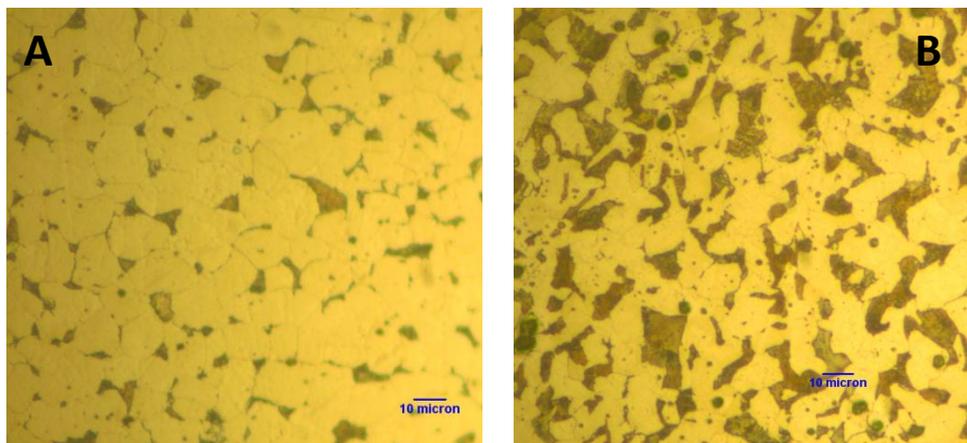


**Figure 1.** *Phase structure of Q235 (A) and HRB335 (B)*

### Polarization curve

In order to understand the formation process of passive film and to determine the passive potential range, a potential scan ranging from -0.6 to 0.65 V is performed. Fig. 2 presents the formation of passive film on Q235 and HRB335 obtained in the simulated concrete pore solution (SPS). It can be seen from Fig. 2 that both electrodes, Q235 and HRB335, exhibit a similar formation process of passive film. A cathodic process takes place when the potential is scanned from point a (-0.6V) to b (-0.41 V) for Q235, and from point a (-0.6 V) to b' (-0.45 V) for HRB335. This cathodic process should be ascribed to the hydrogen evolution reaction, because the experiments were carried out under nitrogen atmosphere and there were no other reducible species in the solution. When potential is scanned from point b (-0.41 V) and b' (-0.45 V) toward positive potential, the current in both cases (Q235 and HRB335 electrodes) increases till the potential approaches point c (-0.18 V). From point c (-0.18 V) to point d (0.65 V) the electrodes reach passive region. Both electrodes, Q235 and HRB335, have similar passive current density of about 4 $\mu A\ cm^{-2}$. The sharp increase of the current density at point d (0.65 V) is ascribed to the $O_2$ evolution, which depends on pH of the solution [13]. The current plateau of the anodic polarization curve indicates the formation of passive film within the potential domain from -0.18 to 0.65 V for both carbon steel electrodes.

Fig. 3 shows the polarization curves of Q235 and HRB335 in the SPS containing 0.4 M chloride ions. Before the measurement, the two carbon steel electrodes were passivated in SPS, in absence of chloride ions, at the potential of 0 V for 60 min. In SPS containing 0.4 M chloride ions, the breakdown of passive films on both electrodes, Q235 and HRB335, occurs at the potential, which is indicated by a drastic increase of current. However, the breakdown potential values of passive

films were different, *i.e.* about 0 V for Q235 and 0.34 V for HRB335. Therefore, the passive film formed on Q235 is more susceptible to chloride ions than the one formed on HRB335 electrode.
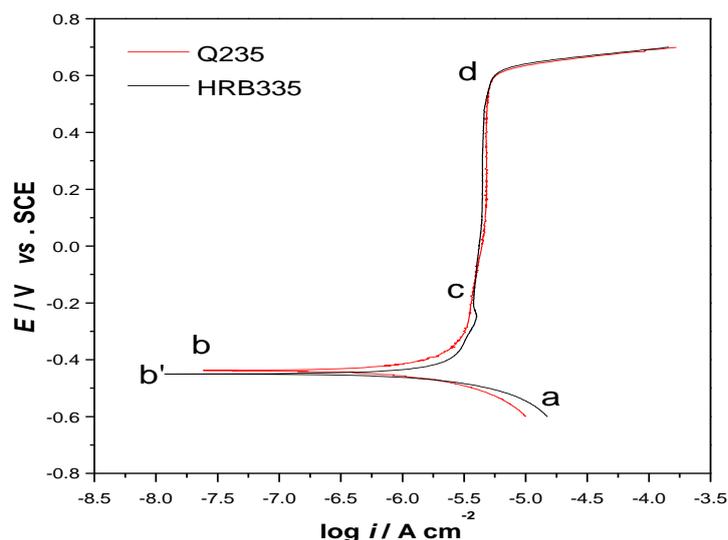


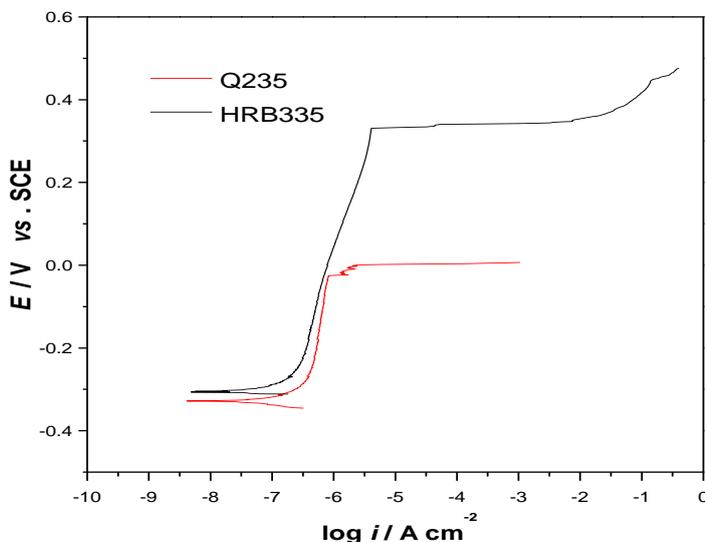**Figure 2.** *Polarization curves of Q235 and HRB335 in SPS in absence of chloride ions (scan rate: 0.5 mV s$^{-1}$).*



**Figure 3.** *Polarization curves of Q235 and HRB335 in SPS containing 0.4 M chloride ions (scan rate: 0.5 mV s$^{-1}$).*

### Electrochemical impedance

Fig. 4 presents the Nyquist plots of passivated Q235 and HRB335 in the SPS containing 0 and 0.4 M chloride ions at open circuit potential. It can be seen from Fig. 4 that two electrodes have similar behavior which does not involve any diffusion process, although there is a significant difference in polarization impedance for the electrodes in the solution with and without chloride ions.

A passivated electrode can be modeled by the equivalent circuit of Fig. 5. In Fig. 5, $R_S$ represents the solution resistance; $R_f$ and $Q$ are the resistance and the space charge layer capacitance of the passive film. The element $Q$ is usually represented by the constant phase element (CPE) in which $n$ is in the range between 0.5 and 1 due to the surface heterogeneity and surface roughness of the passivated electrodes [14]. The impedance of a CPE is given by

$$Z_{CPE} = \left[ y^0 \left( jw \right)^n \right]^{-1} \tag{1}$$
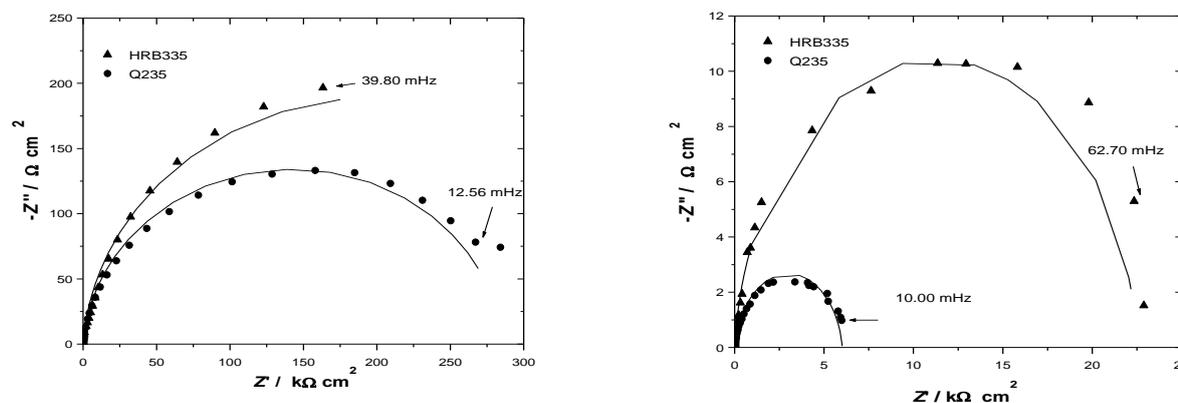
**Figure 4.** *Nyquist plots of passivated Q235 and HRB335 electrodes in SPS: (a) without chloride ions; (b) containing 0.4 M chloride ions*

The capacitance element *Q* (CPE) is pure capacitance when n = 1 and pure resistance when n = 0. The results obtained from fitting with Fig. 5 are shown by solid lines in Fig. 4 and by the data in Table 2. It can be seen from Table 2 that, in the solution without chloride ions, the film resistance ($R_f$) of Q235 is smaller than the one of HRB335, indicating that the passivated Q235 tends to react more easily than the passivated HRB335. When chloride ions are added in the solution, the resistance of the film decreases for both carbon steel electrodes.
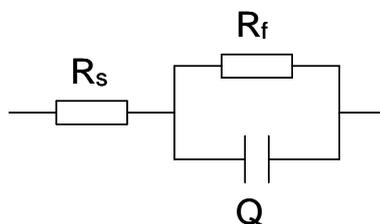


**Figure 5.** *Equivalent circuit for a passivated electrode.*

*Mott-Schottky analysis*

Passive films of most metals behave as semiconductor [15-18]. In the high frequency domain, the Mott-Shottly approach is a good tool for characterizing the semiconducting properties of a passive film [19,20]. When the frequency used for the impedance measurement is high enough, potential dependence of the capacitance of space-charge layer ($C_{sc}$) is expressed by Mott-Schottky relationship [5]:

For n-type semiconductor

$$\frac{1}{C_{sc}^{2}} = \frac{2}{e\varepsilon_r\varepsilon_0 N_D}\left(E - \phi_{fb} - \frac{kT}{e}\right) \tag{2}$$

For p-type semiconductor

$$\frac{1}{C_{sc}^{2}} = -\frac{2}{e\varepsilon_r\varepsilon_0 N_A}\left(E - \phi_{fb} - \frac{kT}{e}\right) \tag{3}$$

where *e* is electron charge ($1.6\times10^{-19}$ C), $\varepsilon_r$ is dielectric constant, taken as 15.6 [17]. $\varepsilon_0$ is the vacuum permittivity ($8.85\times10^{-14}$ F cm$^{-1}$), $N_D$ is donor density, $N_A$ is acceptor density, *E* is the applied potential, $\varphi_{fb}$ is flat-band potential, *k* is Boltzmann constant ($1.38 \times 10^{-23}$ J K$^{-1}$) and *T* is absolute temperature. $N_D$ and $N_A$ can be determined from the slope of the linear relationship between $C_{sc}^{-2}$ and *E*, while $\phi_{fb}$ is obtained from the extrapolation to $C_{sc}^{-2} = 0$.
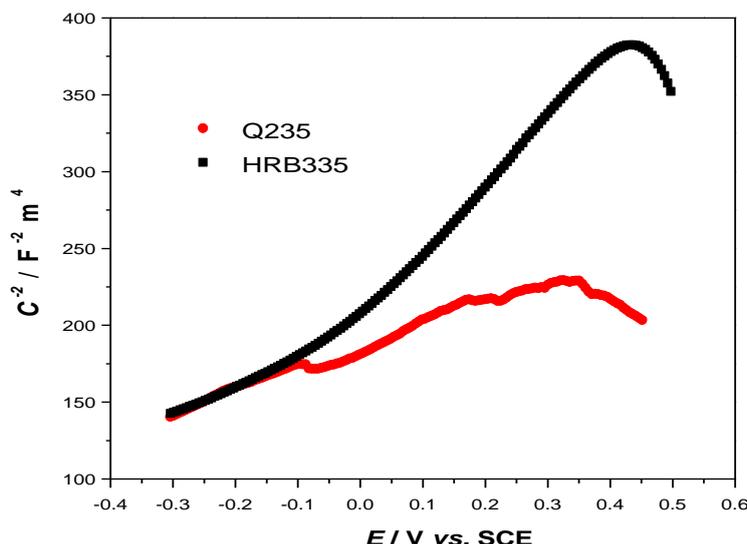
**Figure 6.** *Mott-Schottky plots of passivated Q235 and HRB335 in the SPS containing 0.4 M chloride ions.*

Fig. 6 shows Mott-Schottky plots of passivated Q235 and HRB335 electrodes in SPS containing 0.4 M chloride ions. It can be seen from Fig. 6 that, at the potentials lower than 0.35V, $C_{sc}^{-2}$ increases with increasing the potential. There is a positive linear relationship between $C_{sc}^{-2}$ and $E$ in the potential range from 0 to 0.15 V for both electrodes, indicating that both passive films are n-type semiconductors [4]. The donor densities values calculated from the slope of the linear relationship between $C_{sc}^{-2}$ and $E$ in Fig. 6 are shown in Table 2. It is found that the donor densities values are very high, *i.e.* in the order of $10^{26}$ $m^{-3}$. This order is characteristic of heavily doped and disordered passive films, which was also found by Cheng and Luo ($10^{26}$ $m^{-3} \leq N_D \leq 10^{27}$ $m^{-3}$) [21]. A donor density of a passive film determines its pitting susceptibility. The larger the donor density is, the more susceptible to pitting of the passive film is. The donor density of passive film formed on Q235 is $4.42 \times 10^{26}$ $m^{-3}$, which is higher the one of HRB335 ($2.29 \times 10^{26}$ $m^{-3}$), confirming that Q235 is more susceptible to pitting than HRB335.

**Table 2.** *Fitting results of the experimental data in Fig. 4 and Fig. 6*

| Samples | $C_{NaCl}$ / M | $R_f$ / kΩ cm$^2$ | $Y^0$ /μS cm$^{-2}$ s$^n$ | n | $N_D$ / $10^{26}$ m$^{-3}$ |
|---|---|---|---|---|---|
| Q235 | 0 | 285.3 | 10.95 | 0.9607 | - |
| Q235 | 0.4 | 6.0 | 18.42 | 0.9236 | 4.42 |
| HRB335 | 0 | 402 | 10.81 | 0.9610 | - |
| HRB335 | 0.4 | 22.5 | 12.55 | 0.9512 | 2.29 |

**Conclusions**

Based on the results from phase observation, potentiodynamic polarization, electrochemical impedance measurements and Mott-Schottky analysis of passive films of two carbon steel electrodes, it can be concluded that Q235 is more susceptible to pitting than HRB335. Q235 has a phase structure of ferrite, which tends to form a less stable passive film and thus is more susceptible to chloride ions than HRB335, whose phase structure is pearlite.

## References

[1]   A.A. Almusallam, *Constr. Build. Mater.* **15** (2001) 361-368

[2]   M. Ormellese, M. Berra, F. Bolzoni, T. Pastore, *Cement Concrete Res.* **36** (2006) 536-547

[3]   W.S. Li, J.L. Luo, *J. Mater. Sci. Lett.* **21** (2002) 1195-1198

[4]   W.S. Li, J.L. Luo, *Corros. Sci.* 44 (2002) 1695-1712

[5]   W.S. Li, N. Cui, J.L. Luo, *Electrochim. Acta* **49** (2004) 1663-1672

[6]   W.S. Li, S.Q. Cai, J.L. Luo,  *J. Electrochem. Soc.* **151** (2004) B220-B226

[7]   J. Lu, W.S. Li, J.L. Luo, *Corros. Eng. Sci. Techn.* **43** (2008)  208-212

[8]   W.S. Li, J.L. Luo, *Int. J. Electrochem. Sci.* **2** (2007) 627-665

[9]   A. Pardo, M.C. Merino, A.E. Coy, R. Arrabal, F. Viejo, E. Matykina, *Corros. Sci.* **50** (2008) 823-834

[10]   E.E Abd El Aal, S. Abd El Wanees, A. Diab, S.M. Abd El Haleem, *Corros. Sci.* **51** (2009) 1611-1618

[11]   F. Zhang, J.S. Pan, C.J. Lin, *Corros. Sci.* **51** (2009) 2130-2138

[12]   L. Hamadou, A. Kadri, D. Boughrara, N. Benbrahim, J.P. Petit, *Appl. Surf. Sci.* **252** (2006) 4209-4217

[13]   D. Trejo, P.J. Monteiro, *Cement Concrete Res.* **35** (2005) 562-571

[14]   M. Cai, S.M. Park, *J. Electrochem. Soc.* **143** (1996) 3895-3902

[15]   A.M.P. Simoes, M.G.S. Ferrira, B. Rondot, M. CunhaBelo, *J. Electrochem. Soc.* **137** (1990) 82-87

[16]   G. Cooper, J.A. Turner, A.J. Nozik, *J. Electrochem. Soc.* **129** (1982) 1973-1977

[17]   K. Azumi, T. Ohtsuka, N. Sato, *J. Electrochem. Soc.* **134** (1987) 1352-1357

[18]   U. Stimming, *Electrochim. Acta* 31 (1986) 415-429

[19]   L. Hamadou, A. Kadri, N. Benbrahim, *Corros. Sci.* **52** (2010) 859-864

[20]   F. Di Quarto, M. Santamaria, *Corros. Eng. Sci. Techn.* **39** (2004) 71-81

[21]   Y.F. Cheng, J.L. Luo, *Electrochim. Acta* **44** (1999) 2947-2957